Modelling dynamics of the estuarine turbidity maximum and local net deposition

Roland F. Hesse [1] · Anna Zorndt [2] · Peter Fröhle [1]

Abstract

Net deposition in estuaries is often linked to the estuarine turbidity maximum zones, in which fine, cohesive sediments accumulate due to residual transport by the estuarine circulation and tidal asymmetries. Sediments deposit in fairways or harbours, which creates high maintenance dredging costs and the need for better prediction of dredging hotspots with process-based numerical models. In this paper, a new efficient modelling approach is presented which enables the simulation of the ETM formation, its seasonal dynamics and the local sedimentation. A 3D baroclinic large-scale estuary model with a characteristic sediment fraction with simplified sediment transport properties is used with realistic boundary conditions, but without initial sediment distribution. This approach is referred to as supply-limited, regarding the ETM formation by residual transport. A dynamic equilibrium between residual sediment import from the open boundaries, accumulation and local sedimentation establishes in the model. This is achieved by combining the large-scale supply-limited model with an extended bed exchange formulation (2-Layer-Concept). A model of the Weser estuary is used as case study to reproduce and analyse the ETM formation and the resulting sedimentation simulated with this approach. The results are compared with the equivalent sediment concentration of turbidity measurements and dredging volumes.

Keywords Fine cohesive sediments · Suspended sediment transport · Bed exchange · Supply-limited model approach · 2-Layer-Concept · Sedimentation · Estuarine turbidity maximum (ETM) · Seasonal sediment dynamics · Estuary · Weser

1 Introduction

1.1 Motivation

In many estuaries, an increased sedimentation of predominantly fine, cohesive sediments occurs in the reach of the estuarine turbidity maximum (ETM), leading to an extensive effort with respect to the maintenance of shipways. The ETM is a zone of elevated sediment concentration which causes a

✉ Roland F. Hesse
roland.hesse@tuhh.de

[1] Institute of River and Coastal Engineering, Hamburg University of Technology (TUHH), Denickestraße 22, D-21073 Hamburg, Germany

[2] Federal Waterways Engineering and Research Institute (BAW), Wedeler Landstraße 157, 22559 Hamburg, Germany

correspondingly high turbidity and is often linked to increased sedimentation. The formation of ETMs can be essentially explained by different residual (tidal averaged net) transport mechanisms in the mixing zones of estuaries (Burchard et al. 2018) in combination with the specific transport behaviour of fine, cohesive sediments. The resulting tidal resuspension-deposition cycles generate a residual transport leading to an accumulation of these sediments (van Leussen 1994, 2011). The residual transport fluxes can be the result of the estuarine circulation and (additional) tidal asymmetries. The estuarine circulation in terms of a residual flow in the lower water column establishes mainly due to an internal density gradient (gravitational circulation) as well as asymmetries in vertical mixing (strain induced periodically stratification, SIPS), both induced by the occurring salinity gradient and stratification in estuaries (Dyer 1973; Simpson et al. 1990; Jay and Musiak 1994; Geyer and MacCready 2014). Besides, these baroclinic processes further tidal asymmetries can also be sufficient to generate a residual transport (Allen et al. 1980; Dyer 1988; Brenon and Le Hir 1999; Burchard et al. 2018):

In the Weser estuary in northern Germany (Fig. 1), the formation of the ETM can be explained by the establishing

estuarine circulation as well as additionally occurring asymmetries in mixing. Maintenance dredging hotspots coincide with the seasonally shifting ETM location. Dredging is necessary due to siltation of fine, mainly cohesive sediments in the navigation channel. Field studies show that a highly concentrated suspension (fluid mud) is formed at slack tide in this reach, leading to net deposition and the subsequent need for dredging. Due to the high costs related to dredging and disposal of fine and sometimes even contaminated material, modelling and forecasting dredging hotspots and the underlying dynamics of estuarine turbidity maxima has become an important modelling task for authorities and consultancies.

The transport behaviour of cohesive sediments is in general very complex due to the inter-particulate binding and depends on numerous parameters and processes (Berlamont et al. 1993). This can result in a temporally and spatially highly variable settling and bed exchange due to flocculation, formation of fluid mud and eventually consolidation or a new resuspension and erosion. These processes can be present in tidal waters at the tidal scale (Winterwerp and van Kesteren 2004). The erodibility of cohesive sediments is not a constant sediment property but depends on several factors, such as the deposition history and the bed structure (Black et al. 2002; Grabowski et al. 2011). Besides, biological processes can play an important role, but reliable quantification of these

processes is still not possible (Black et al. 2002). Detailed settling and deposition or bed exchange model approaches exist (e.g. Le Hir et al. 2011; Sanford 2008; Winterwerp 2002) but are not yet applicable for all conditions (e.g. fluid mud) without restrictions to large-scale engineering-type sediment transport simulations due to the complexity and often limited measured data for calibration. Therefore, simple formulations have to be used which do allow for simulation of large-scale sediment transport processes and accumulation despite neglecting of the detailed reproduction of local bed structure and composition. In van Kessel et al. (2011), a new bed exchange parametrization concept is presented, which is referred to as 2-Layer-Concept. The bed exchange is simplified with two layers to reproduce erosion fluxes for different forcing regimes to enable the simulation of seasonal sediment dynamics.

Already Lang (1990) and Malcherek (1995) have set up models to reproduce sediment dynamics in the ETM of the Weser. However, it was stated that the model was not able to reproduce the ETM dynamics over a long time (> month) as sediment availability was mainly dependent on local erosion. Sediment accumulation could not be reproduced as model extent and computational period were too small due to computational limitations. In a more recent study (van Maren et al. 2011), it was emphasised that the local fine sediment
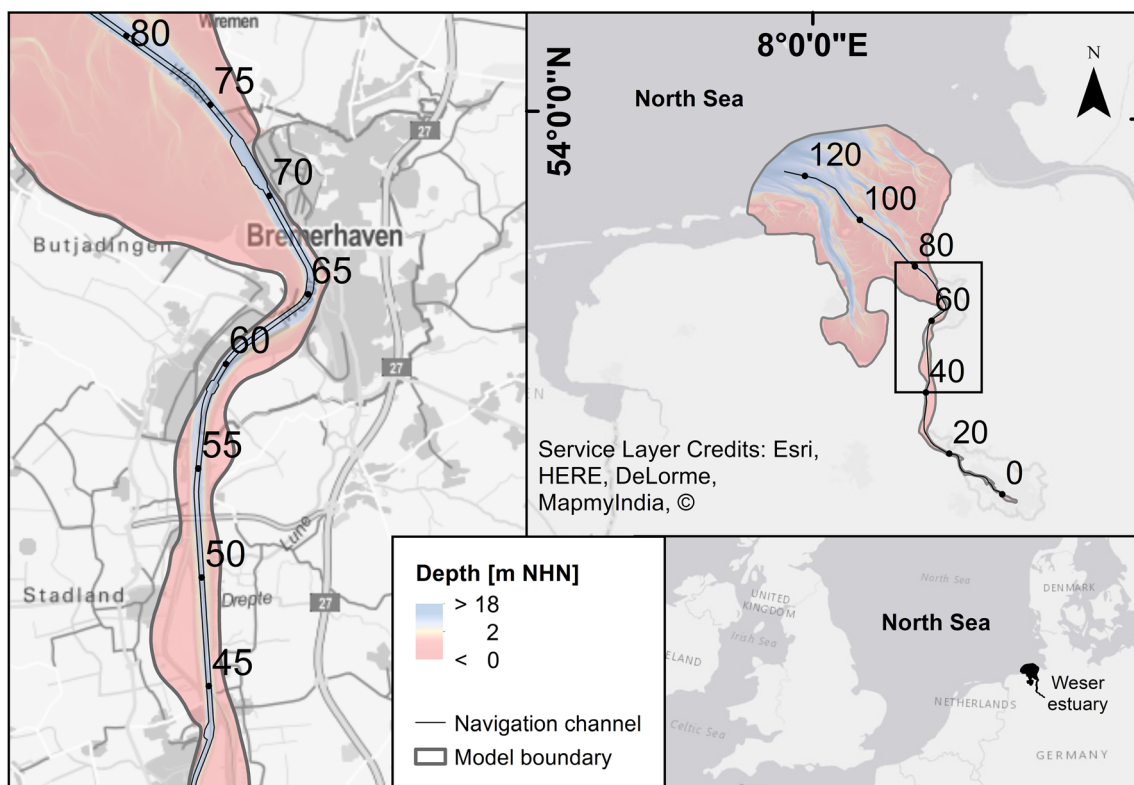

Fig. 1 Location of the Weser estuary (bottom right), Weser estuary model domain (top right) and study focus area (left). Indicated are kilometres along the navigation channel and depths below chart datum m NHN. In the Weser estuary, the chart datum NHN corresponds roughly to the mean sea level (Hesse 2018; data source BfG 2014a; Heyer and Schrottke 2013)

dynamics in estuaries and especially in the reach of an ETM are rather controlled by the residual transport and dynamic accumulation of sediments than merely local erosion. Thus, sediment availability in terms of accumulated erodible sediment deposits controls the local sediment dynamics. Hence, when running a sediment transport model with an initial distribution of sediments especially for a short simulation time, it is a challenge to calibrate the model and to prove if the model correctly reproduces the physical processes leading to the ETM formation or if the modelled sediment concentrations stem from local erosion of the initialized sediment bed. In complex estuary models with realistic boundary conditions and a complex sediment initialization, this is usually overcome by a morphodynamic "spin-up" period to readjust the initial distribution of sediments to the model physics with the aim that the results are then no longer dependant on the initialization (see also van der Wegen et al. 2011). A recent example of this is the study of Grasso et al. (2018) and Schulz et al. (2018), who presented a sophisticated and complex baroclinic 3D estuary model of the Seine estuary. The sediment dynamics are computed by four sand and one mud fraction, which are initially specified in the bed according to sediment distribution measurements. For the bed exchange, a detailed multilayer bed exchange model is applied which takes an increased erosion resistance of sand-mud mixtures and consolidation into account. They use a model initialization phase of 1 year and could show that the model was then able to reproduce short-term and long-term sediment dynamics very well. This however is computationally expensive.

1.2 Objectives

The general aim of this study is the test and evaluation of a new modelling strategy for an improved and efficient simulation of the seasonal dynamics of fine, cohesive sediments in estuaries with simplified formulations and currently available hydro-numeric modelling methods. The focus lies on the formation of the ETM and its dynamics behaviour as well as the resulting sedimentation independently of the initial conditions. The sediment source is considered explicitly in terms of analysing the sediment transport and balances. The ETM is supposed to evolve in the model due to the balance between residual transport into the estuary, local net deposition and the establishing local sediment availability. Thus, the modelled ETM is the result of a dynamic equilibrium as it is in nature. The particular focus lies on reproducing the sediment mass balances and the seasonal turbidity levels. The appropriate reproduction of the seasonal dynamics of the mixing zone in the model and the seaward sediment source at the sea boundary are crucial due to the influence on the residual sediment transport. However, the detailed analyses and evaluation of the underling hydrodynamic transport mechanisms are not part of this study. Furthermore, the vertical distribution of

suspended sediment concentration and the actual bed structure are chosen not to be modelled in detail. The model approach is tested for a specific estuary as case study to be able to compare the achieved results with measurements, documented dredging activities and the results of previous studies.

Summing up, the following two basic dominant processes shall be simulated with the model to reproduce the seasonal dynamics and sedimentation behaviour of the cohesive sediment fraction with respect to the introduced findings:
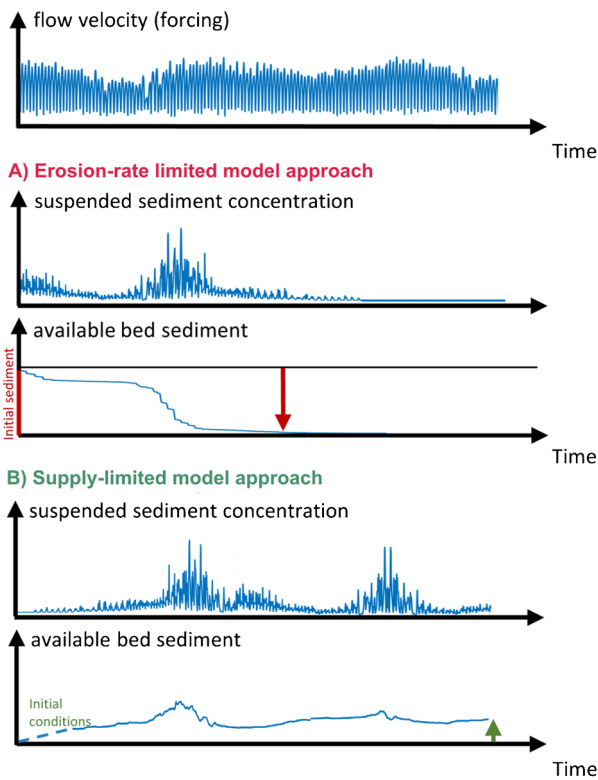
1. Formation of the ETM in the model by sediment transport from the sea and residual accumulation processes due to estuarine circulation and tidal asymmetries induced by the modelled salt distribution rather than instantaneous local erosion (supply-limited model approach, Fig. 2b)
2. Sedimentation in the reach of the ETM according to documented dredging (Fig. 2c) due to the following:

(a) A high settling/deposition flux of the accumulated sediments (sediment availability due to supply-limited approach) and
(b) An increasing erosion resistance of deposited sediments (erosion reduction) for conditions with temporarily high suspended sediment concentrations at the bed.

Only essential processes for the seasonal ETM dynamics and balances are considered in the model setup to keep it simple and efficient. Many relevant processes are still not well understood and have to be parameterized in a simplified way. Also, sufficient measured field data for appropriate initial conditions often cannot be obtained. Therefore, only one characteristic sediment fraction with simplified sediment properties and bed exchange is used without an initial sediment distribution in the model. The supply-limited model approach (van Maren et al. 2015) and the 2-Layer-Concept by van Kessel et al. (2011) are chosen for this purpose to enable a simplified process-based simulation of the ETM. The unique outline of this study is the combination of these concepts, its adaption for ETM conditions and its consistent application for an entire estuary model with only one characteristic sediment fraction. This allows for an efficient simulation of ETM dynamics in spite of the underlying complex and partly unclear detail processes on different scales. The reduced computational effort due to these simplifications and the use of currently available modelling methods are promising for a feasible operational application on practical sediment management and maintenance issues.
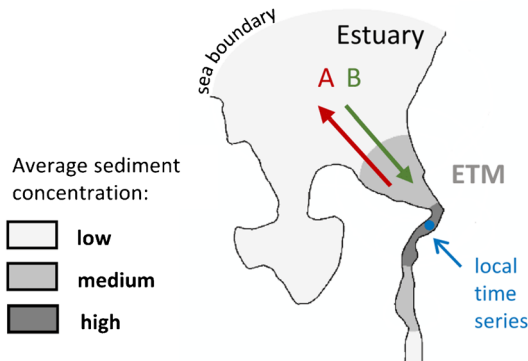
1.3 Model concept

Figure 2 shows a conceptual sketch to illustrate the key ideas of the modelling concept. In traditional modelling approaches
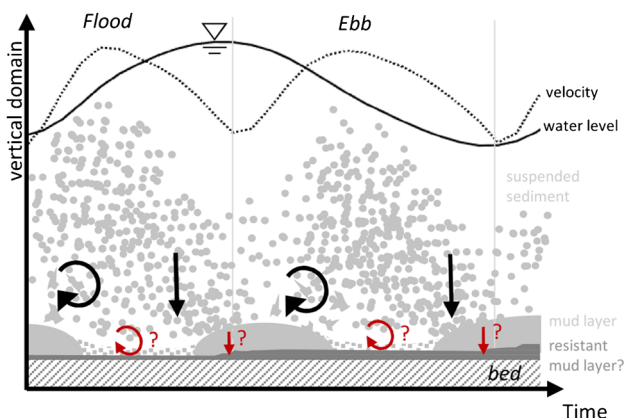
a Sediment transport modeling approach

flow velocity (forcing)

Time

A) Erosion-rate limited model approach

suspended sediment concentration

Time

available bed sediment

Time

B) Supply-limited model approach

suspended sediment concentration

Time

available bed sediment

Initial
conditions

Time

b Large scale residual sediment transport

Estuary

A B

ETM

sea boundary

local
time
series

Average sediment
concentration:

☐ **low**
▨ **medium**
▩ **high**

c Bed exchange concept

Flood   *Ebb*

velocity

water level

suspended
sediment

mud layer

resistant
mud layer?

bed

Time

◀ **Fig. 2** Conceptual sketch for applied modelling approach. **a** Sediment transport modelling approach: erosion-rate limited approach (A) versus supply-limited (B) (after van Maren et al. 2011), illustrated by time series of flow velocity, suspended sediment concentration and available bed sediment at the location shown in **b**. **b** Resulting direction of large-scale residual transport for model approaches (A) and (B). **c** Bed exchange concept (adapted from Hesse 2018)

(e.g. Lang (1990), Malcherek (1995) for the Weser or recently Grasso et al. (2018) for the Seine), an initial sediment distribution is specified in a sediment transport model and sediment parameters are calibrated according measured concentrations. According to van Maren et al., this can be denoted as an *erosion-rate limited model approach* (A), in which the local suspended sediment concentration (ssc) is controlled by the erosion rate of the initially specified available sediment. This approach might conceal errors in the large-scale hydrodynamics or the exchange parameter settings and might result in wrong sediment transport balances. While short-term ssc patterns may seem realistic, a long-term equilibrium is not reached, resulting in a continuous loss of sediment and a continuous reduction of the initial sediment budget as shown in Fig. 2a. This could lead to fading of the modelled ETM and can be contrary to the observed behaviour in nature. This problem, which can appear in traditional approaches, could be overcome by using a *supply-limited modelling approach* (B) for calibration as suggested by van Maren et al. (2011): suspended sediments are only specified at the open boundaries and not by initialization of the bed layer, so that a stable ETM only evolves if a residual sediment import establishes in the model (Fig. 2b). Accordingly, the available sediment depends dynamically on the residual import from the boundaries (comp. van Maren et al. 2011, 2015). However, this depends on the parameterization of the bed exchange in combination with the settling parametrization in the advection-diffusion equation. Thus, this approach is used to determine parameters, leading to a dynamic equilibrium between residual import, resulting local ssc due to resuspension and ETM formation as well as sedimentation in the model.

To reproduce the residual transport and sediment dynamics simulation of realistic large-scale three-dimensional hydrodynamic sediment transport with appropriate boundary conditions is combined with a simplified parametrization of settling and bed exchange processes. To reproduce the tidal average sediment dynamics, the tidal cycle has to be resolved with respect to the residual transport (van Leussen 1994, 2011; Jay and Musiak 1994). The settling is parameterized with characteristic constant settling velocities for the studied problem (Winterwerp and van Kesteren 2004). To be able to model the sedimentation for the resulting conditions with high sediment availability, different exchange regimes for the bed exchange have to be taken into account (Fig. 2c): in general, resuspension and transport during the tidal cycle results in long-term residual transport and eventually in the formation

of the ETM (Fig. 2b). For conditions with high deposition fluxes and consequently presence of highly concentrated suspension at the bed, as occurring in the ETM, an erosion resistant layer due to reduced erosion and/or stabilisation processes can establish which leads to long-term sedimentation (Fig. 2c). To parameterize the described processes in a simplified way, the 2-Layer-Concept is adopted.

A drawback of using only one fraction with a constant settling velocity is that the vertical distribution cannot be reproduced accurately (Winterwerp 2002). Anyway, the aim of this approach is to reproduce the sediment dynamics in terms of seasonal variations and balances in the model. Furthermore, the simplified parameter setting enables the application of available modelling methods with reasonable computational resources and effort as well as the calibration of the model with available measured data.

2 Method

To simulate the three-dimensional hydrodynamic currents and transport of constituents (salt and sediment) and the bed exchange of sediments, delft3d (Lesser et al. 2004) is applied. The shallow water equation is solved with Boussinesq and hydrostatic pressure assumption and considering the Coriolis force. The vertical velocities are computed from the continuity equation. For turbulence closure, the k-ε model is used. The density influence of the transported constituencies on the fluid density is taken into account. The transport of suspended sediments is calculated by the three-dimensional advection-diffusion transport according to Eq. 1 (mass-balance), where c is the suspended sediment concentration (ssc), u, v and w are the Reynolds averaged velocities in corresponding directions x, y and z and k_v and k_h are the diffusion coefficients in vertical and horizontal directions respectively. The vertical diffusion k_v is calculated by the modelled turbulent viscosity, while for the horizontal diffusion a constant coefficient k_h is used.

$$\frac{\partial c}{\partial t} + \frac{\partial uc}{\partial x} + \frac{\partial vc}{\partial y} + \frac{\partial (w-w_s)c}{\partial z}$$
$$-\frac{\partial}{\partial x}\left(k_h \frac{\partial c}{\partial x}\right) - \frac{\partial}{\partial y}\left(k_h \frac{\partial c}{\partial y}\right) - \frac{\partial}{\partial z}\left(k_v \frac{\partial c}{\partial z}\right) = 0 \quad (1)$$

Bed load transport is not modelled as the focus lies on the suspended sediment transport of the cohesive fraction. A constant settling velocity w_s is used for this purpose which can be interpreted as a characteristic parameter for the residual transport in the system (comp. Winterwerp and van Kesteren 2004, p. 122). Besides the suspended transport in the water column, the 2-Layer-Concept by van Kessel et al. (2011) is applied for the bed exchange to be able to reproduce the described objectives. This concept extends the bed exchange parametrization of *Ariathurai-Partheniades* with an additional fast responding

upper fluff layer (F). This concept has already been applied to model the seasonal variation of suspended sediments in the Markermeer (van Kessel et al. 2009) and to model the seasonal sediment dynamics in the Ems estuary (van Maren et al. 2015). It is important to notice that the fluff layer itself is dimensionless. The aim of the concept is to reproduce the seasonal bed exchange fluxes for different forcing regimes in a simple, parametrized way. The five equations (Eqs. 2–5; van Kessel et al. 2011) are used to calculate the fluxes at the bed (Fig. 3):

$$D_{(F)} = w_S c_b \quad (2)$$

$$E_F = M_F \begin{cases} \tau_b - \tau_{cr,e,F} & |\tau_{cr,e,F} \leq \tau_b \\ 0 & |\tau_{cr,e,F} > \tau_b \end{cases} \quad (3)$$

$$M_F = \min(m_F M_1, M_0) \quad (4)$$

$$B_F = \min(m_F B_1, B_0) \quad (5)$$

$$E_B = M_B \begin{cases} \dfrac{\tau_b}{\tau_{cr,e,B}} - 1 & |\tau_{cr,e,B} \leq \tau_b \\ 0 & |\tau_{cr,e,B} > \tau_b \end{cases} \quad (6)$$

Deposition D is calculated by the specified settling velocity w_s and the modelled concentration at the bed c_b (continuous deposition). This leads to an increase of the mass m_F in the fluff layer. The sedimentation flux into the bed layer B_F and the erosion flux E_F are modelled with first-order dependencies on m_F, the parameters for the exchange rates ($M_{1,0}$; $B_{1,0}$) and modelled and specified critical bed shear stresses (τ_b, $\tau_{cr,e}$) resulting in simple mass balances for the dimensionless fluff layer. The modelled shear stress at the bed (τ_b) is calculated as a function of a modelled flow velocity at a fixed reference height above the bed level. The erosion flux from the bed (E_B) is calculated according to the classical *Ariathurai-Partheniades* parametrisation. This formulation is applied only to calculate the bed exchange fluxes dependent on modelled sediment availability (c_b) and forcing (τ_b). The actual structure of the bed is not modelled deliberately due to the mentioned complexity of the involved processes which are not known in detail. Consequently, a potential impact of the mud layer on the hydrodynamics is not taken into account in the model. For the approach described here, this concept is adopted to reproduce the short-scale tidal dynamics of sediments in the water column and the resulting residual transport from the boundaries as well as a partly increasing erosion resistance of the deposited sediments in areas with a temporally concentrated suspension at the bed. Hence, the ETM formation as well as long-term net deposition in the navigation channel at the ETM can be simulated. The bed exchange formulation of the 2-Layer-Concept (Eqs. 2–5) is consistently used for the whole model domain. Figure 3 shows a conceptual, process-orientated overview of the model focusing on the vertical sediment transport and exchange by the 2-Layer-Concept formulation on the grid element scale (left-hand side) as well as its implication on the
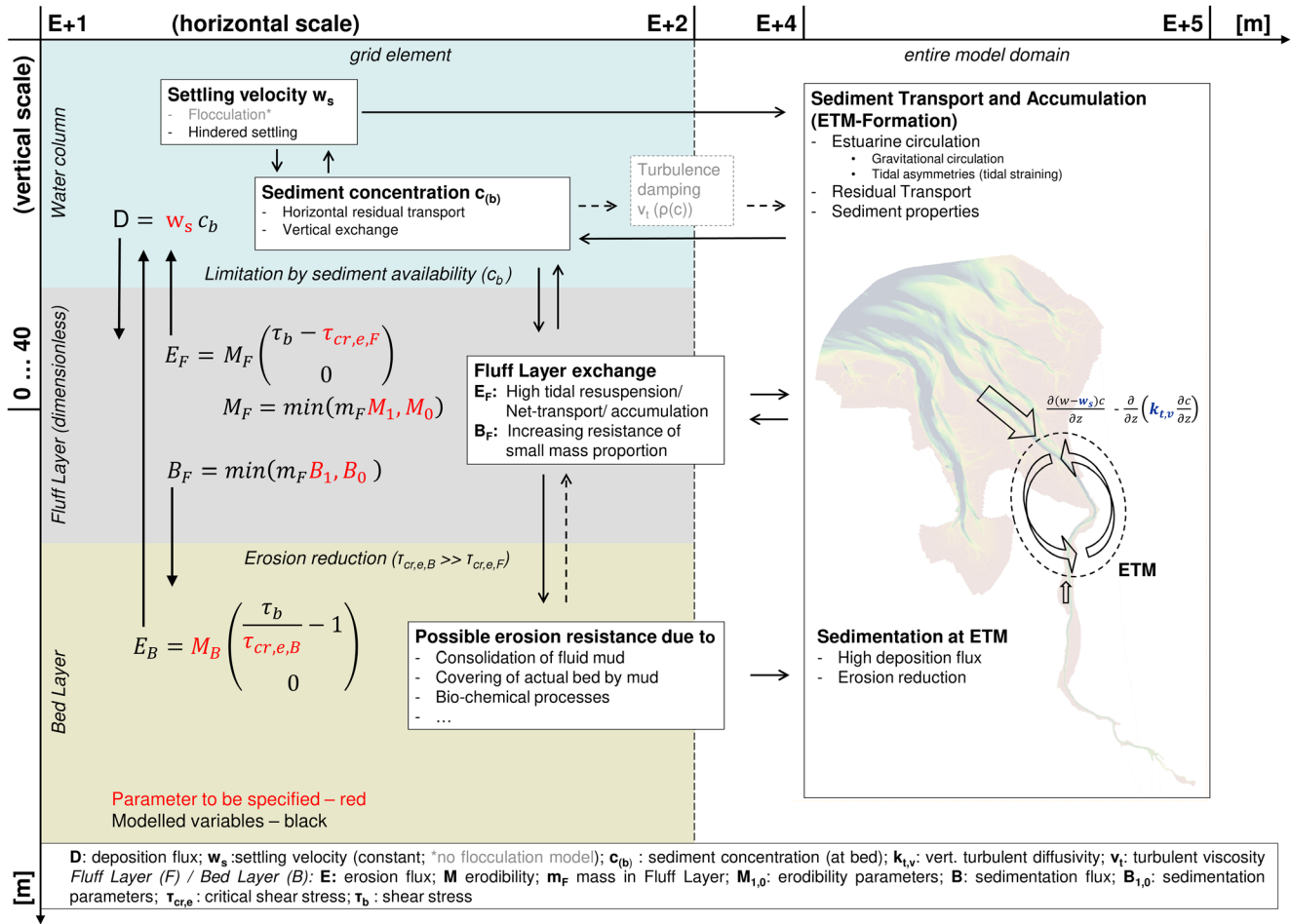
Fig. 3 Conceptual, process-oriented model overview regarding the vertical sediment transport and bed exchange on the grid element scale and the resulting impact on the entire large (horizontal)-scale residual sediment transport in the model (Hesse 2018)

horizontal large-scale long-term residual transport and accumulation processes (right-hand side) due to modelled hydrodynamic tidal flow and salt distribution. Besides the residual current, the accumulation and formation of a stable ETM in the model can be explained essentially by the dynamic balance between modelled turbulent vertical diffusion (k_v) and the specified settling velocity w_s according to the corresponding terms in Eq. 1.

To test the presented modelling approach, a model of the Weser estuary with realistic boundary forcing is set up for comparing the simulation results with equivalent ssc of optical turbidity measurements. To be able to show the seasonal variation in sediment dynamics, a 1-year period is studied.

3 Application to the Weser estuary

3.1 Regional setting

The Weser estuary is situated in the north-west of Germany. It is the tidally influenced transition water of the Weser River and the North Sea (German Bight). Figure 1 shows the

location of the estuary, the course and kilometre indication of the navigation channel, the extent of the study area and the selected model domain respectively. An enlarged detail shows the focus area of the study between km 40 and km 80 of the navigation channel. The inner estuary (km 0 to 65) has a channel-like course till the city of Bremerhaven at km 65, while the outer estuary (km 65 to 120) is funnel-shaped with two main channels and extensive tidal flats. The course of navigation channel is stabilised by several engineering measures (e.g. sheet pilings, groynes and dredging) with a maintained depth of about 12 m in the inner and 16 m below chart datum in the outer estuary. In the south-west, the Jade Bight, a bay without noteworthy fresh water inflow, is part of the estuary system. The mean river discharge of the Weser is 326 m^3/s and can vary between 116 and 1200 m^3/s on long-term average. The mean range of the semidiurnal tide is 2.8 m in the outer estuary, but reaches 4.1 m at the tidal weir in the south of the city of Bremen (km 0). Thus, the estuary can be classified as hypersynchronous and meso-macrotidal. Spring-neap variations are within the range of 1 m on average. Due to the fresh water inflow, a brackish mixing zone (2...20 ppt)

establishes between Weser km 45 and 70 at low slack water and between Weser km 60 and 90 at high slack water depending on hydrological conditions. In general, the estuary is vertically well-mixed, though temporary vertical stratification occurs (Lange et al. 2008; Grabemann et al. 1997).

3.2 Sediment dynamics

In the reach of the mixing zone, an ETM is observed. The typical averaged position can be located between Weser km 30 and 90, but depends strongly on the hydrological conditions (essential river discharge) and is associated with the mixing zone (Kösters et al. 2014; Grabemann et al. 1995). The formation of the ETM can be explained by tidal asymmetries, estuarine circulation and resulting residual sediment import from the sea, whose actual magnitude is not known (Grabemann and Krause 2001). Besides gravitational circulation, tidal straining due to asymmetric vertical mixing can be identified as the main contribution to the estuarine circulation and ETM formation in the Weser (Lang 1990). This is in accordance with studies of Burchard and Hetland (2010) on periodically stratified estuaries. In general, the ssc is in the range of approximately 0.05 kg/m^3, but in the Weser it reaches more than 0.25 kg/m^3 on average in the ETM (Grabemann and Krause 2001). Field studies (applying hydroacoustic measurements) show that a high concentrated suspension occurs temporarily in the reach of the ETM (Schrottke et al. 2006). The temporary mud layer can exceed 10 kg/m^3 (fluid mud), reach a magnitude of metres and show a distinct vertical structure with different rheological behaviour (Papenmeier et al. 2013), but is in general resuspended by the successive tidal current. It is assumed that a certain amount of the mud layer is not resuspended, can develop an increasing erosion resistance and forms stable deposits, which leads to sedimentation in spite of relatively high shear stresses in the navigational channel. Even though the stabilisation processes are not known in detail, the observed erosion resistance is referred to the temporary formation of the mud layer forming due to the increased sediment deposition flux in the ETM at slack tide (Schrottke et al. 2006). In addition, it can be shown that occurring mobile mud layers in reaches with a smooth bed seem to be more resistant to entrainment as mud in troughs of large dunes (Becker 2011). In the inner estuary (km 0 to 65), sediments range from fine to medium sands in general. Bed forms with distinct dunes and ripples are present. An exception is the reach between km 51 and 65, where very fine sediments (silt) with a high organic load and cohesive behaviour predominate on a mainly flat bed. This reach coincidences with the typical frequent ETM location. On average, 80% of all dredged sediments in the inner estuary accrue in this reach. The proportion of fine sediments (< 0.2 mm) can reach 90% of the dredged sediment fractions and sedimentation of these sediments takes place in the navigation channel.

In 2009, the total volume of dredged sediments summed up to approx. 2.3 m. m^3/a for example, which is equivalent to approx. 3.6 m t/a. For other years, a similar magnitude and behaviour is reported (BfG 2014b). The magnitude of the dredged sediments cannot be explained by the sediment load of the river, which is approximately more than one magnitude lower.

3.3 Model setup and data

A three-dimensional model of the Weser estuary is set up as realistic case study to compare model results with available measurements. The spatial domain of the model of the Weser estuary has an extent of about 100 km from north to south (comp. Fig. 1) to model the large-scale sediment transport. The domain is discretized by about 15,000 elements on a curved linear grid with 10 vertical layers (sigma layer with relative magnitude of water depth of 20, 20, 15, 12, 10, 8, 6, 4, 3 and 2% from surface to bed). The horizontal resolution varies between 50 and 1400 m equivalent element length. The inner estuary (km < 65) has a finer resolution while the grid in the outer estuary is coarser. A bathymetry from 2012 (BfG 2014a; Heyer and Schrottke 2013) is interpolated on the grid. According to the Courant criterion and the spatial resolution, a simulation time step of dt = 25 s is used. The simulation period covers the year 2009 with corresponding boundary conditions.

Only essential processes are included into the model to keep the model as simple as possible at the current stage. A wind time series measured at one location in the outer estuary (ALW, approx. km 115; DWD 2013) is applied for wind shear stress as boundary condition at the water surface. The influence of waves is not included. At the river boundary in the south, measured time series of discharge, salinity and ssc (WSV 2014, 2015) are used as boundary values. The salinity in the river Weser amounts to up to approx. 1 ppt due to mining. For the sea boundary in the north, realistic water levels and salinity are extracted from a larger model of the German Bight provided by the German Federal Waterways Engineering and Research Institute (BAW 2012). To ensure that the ETM does not evolve merely due to local erosion, no initial sediment distribution is provided and sediment concentrations are only specified at the open model boundaries. A constant boundary value for ssc of 0.1 kg/m^3 is found for the sea boundary to reproduce the sediment dynamics the estuary correctly. This is in the range of reported concentrations in the Weser (Grabemann 1991) and should be understood with regard to the focus area according to the model supply-limited approach as a general sediment source rather than an actual boundary concentration. The modelled sediment concentration in the water column outside the ETM is considerably lower. Besides, only one characteristic sediment fraction with a constant settling velocity w_s = 2 mm/s is used to simulate the

sediment transport and distribution in comparison to observed turbidity levels and dredged sediment mass. Due to the fact that the navigation channel in the estuary is intensively maintained and as the focus of the study lies on the sediment balance rather than the actual morphological evolution, morphostatic simulations with a fix bed level are performed. The bed roughness was adjusted for calibration of the hydrodynamics and varies in the longitudinal course of the estuary between $z_0 = 0.015$ m (outer estuary) and 0.1 m (inner estuary).

The bed exchange parameters are presented in Table 1. The critical bed shear stress of the bed layer ($\tau_{cr,e,B}$) is set relatively high, if considered as pure sediment property due to two aspects: for the application of the 2-Layer-Concept for ETM conditions, this parameter can be understood in terms of effective erosion reduction of deposited sediments in nature. This reduction can be due to the stabilisation processes as consolidation, as well as a potential reduction of effective shear stress due to the occurring mud layer above the actual bed, which is not directly reproduced in the model. Furthermore, artificial sediment extraction from the system by dredging is not considered in the model so far. Thus, it is not yet possible to determine the exchange behaviour of the lower bed layer due to the intensive artificial impact of dredging. Accordingly, the bed layer can be considered as a buffer to balance processes, which are not resolved with the present model setup.

The simulation results are compared to equivalent ssc of optical turbidity measurements (WSV 2015) and documented dredging volumes (BfG 2014a). For the conversion between measured turbidity [NTU] and equivalent ssc [kg/m^3], a linear relationship is used (Maushake and Grünler 2015). Research indicates that the relationship between turbidity and ssc might not be strictly constant in the tidal cycle, e.g. due to a changed composition of sediments (Downing 2006; Holliday et al. 2003). Thus, the measured turbidity might not fully represent the actual short-term variation of equivalent sediment concentration in nature, though the tidally averaged, seasonal trend in concentration or turbidity levels can be expected to be comparable.

Table 1 Overview of applied bed exchange parameters

Bed exchange parameter name		Symbol	Unit	Value
Critical shear stress	Fluff layer	$\tau_{cr,e,F}$	N/m^2	1.0 E− 2
	Bed layer	$\tau_{cr,e,B}$	N/m^2	6.0
Deposition parameters	Fluff layer	B_0	kg/m^2/s	1.0
		B_1	1/s	1.0 E− 6
Erodibility parameters	Fluff layer	M_0	s/m	1.0 E− 1
		M_1	ms/kg	1.0 E− 1
	Bed layer	M_B	kg/m^2/s	1.0 E− 4

4 Results

## 4.1 Hydrodynamics, salinity, estuarine circulation and tidal asymmetries

Water levels and salinity along the navigation channel can be reproduced with the model adequately for the whole simulation period in comparison to measurements at five monitoring stations in the focus area with root mean square errors smaller than 25 cm (3 %) and 3 ppt (10 %), where the relative percentage refers to the total absolute variation at the corresponding location. The location and especially the seasonal shift of the mixing zone (2…20 ppt) can be reproduced quite well with the model in accordance with the measurements. However, the average mixing zone location is slightly shifted seawards by between 5 and 10 km. Regarding the model extent of more than 120 km, this shift can be considered minor. The seasonal shifting is slightly delayed temporarily respectively. Figure 4 exemplarily shows the measured and modelled water levels (wl) and salinity (sa) at measuring station NUF, km 55.81, which is frequently in the centre of the ETM.

Due to the modelled salt distribution and temporary stratification, an estuarine circulation establishes in the model. The estuarine circulation is investigated qualitatively in Fig. 5, which shows the resulting modelled flow and mixing at km 55 and 75, which is frequently the seaward boundary of the ETM. The residual flow structure is illustrated by the mean horizontal velocity component (vhn) through the cross section of the channel and the average salinity at km 75. A residual flood directed flow is establishing in the lower part of the channel in the outer estuary (Fig. 5a) reaching to the landwards tip of the mixing zone (not shown). The lateral distribution of the residual flow profile is ascribed mainly to the channel geometry. Figure 5b, c exemplarily shows the asymmetry in vertical mixing by the variation of k_v, which is plotted for four tidal cycles over relative water depth with local water level and depth averaged horizontal velocity component. Different types of asymmetries in mixing are present. In general, the mixing is stronger at km 55 (Fig. 5c), but there is not a strong asymmetry between the mixing during flood and ebb current. There is, however, an asymmetry in the slack time durations, which can be seen in a longer period of reduced vertical mixing during flood slack. At km 75 (Fig. 5b), there is much stronger mixing during flood than during ebb, but less mixing in general. These analyses show that there are asymmetries in mixing on the tidal scale, but also strong spatial differences in mixing.

4.2 Sediment dynamics, transport and ETM formation

The following presented results refer to thirteen simulations ($S<…>$, see Table 2), in which mainly the settling velocity and the boundary values are varied. Simulation S0346 is

Fig. 4 Measured (M001) and modelled (S0346) data at station NUF, km 55.81. **a** Tidal average and envelope (12.5 h moving filter) of water level (wl) and salinity (sa) for 2009. **b** Resolved time series from Oct. 17 to Nov. 3 2009 (spring-neap variation indicated by full (black circle) and new (white circle) moon) (Hesse 2018)
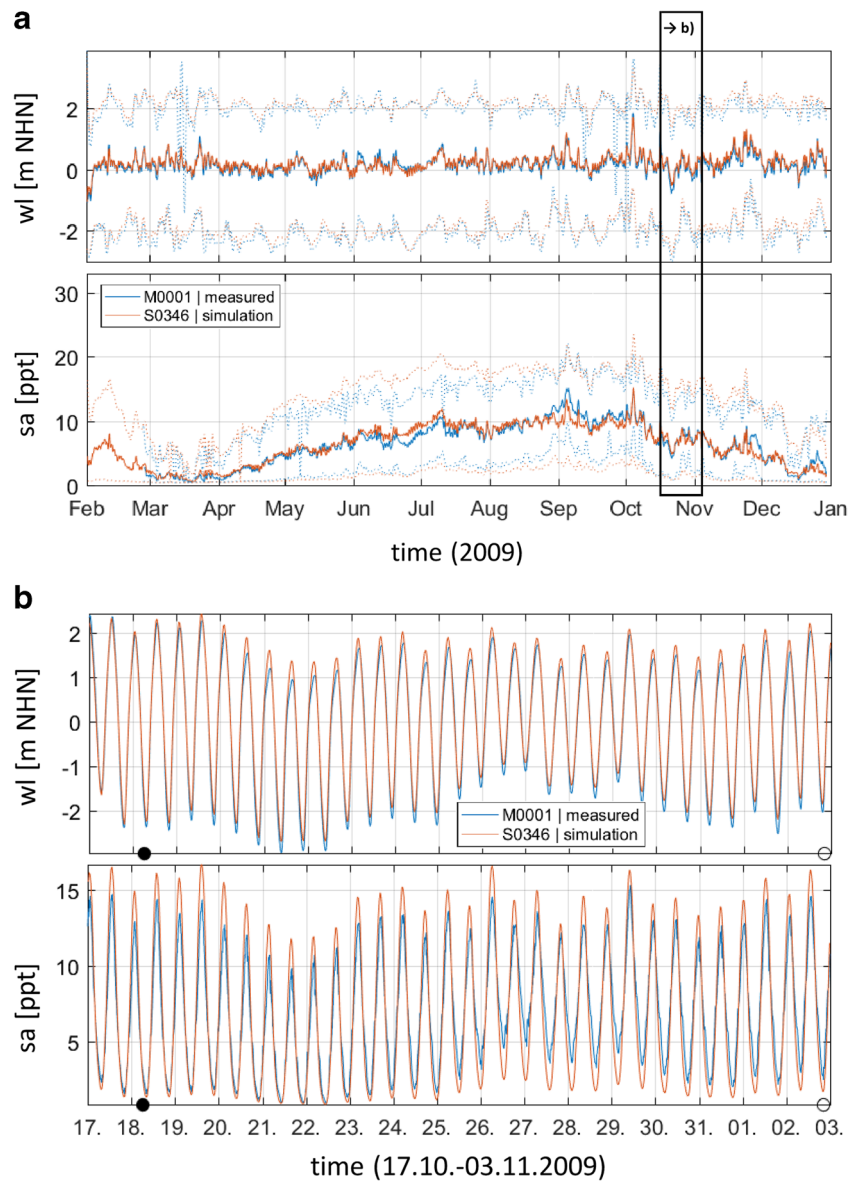
considered as the best case and reference run. The results of this simulation are compared to the measurement data (M0001).

The model succeeds to reproduce the dynamic formation of an ETM (Fig. 6). This is due to the shown residual flow patterns and mixing asymmetries. After only about 2 weeks, accumulation of fine sediment in the ETM zone occurs. This transport time and magnitude seems to be plausible as continuous dredging up to several times a month has to be applied.

Only for certain settling velocities, an import in the magnitude of the documented dredging (BfG 2014b) is reproduced (Fig. 7a). These are in the upper range of measured median settling velocities in different estuaries ($w_s \approx 0.0006\ldots$ 10.0 mm/s reported in Pejrup and Mikkelsen 2010) and in the Weser estuary ($w_s \approx 0.006\ldots1.0$ mm/s reported in Mueller and Puls 1996). The higher velocities ($w_s = 1\ldots$

5 mm/s) are equal to measured settling velocities of macroflocs in the Ems estuary (van Leussen 2011, 1994). The highest residual sediment import is modelled for $w_s =$ 1 mm/s, whereat the seasonal transport intensity is strongly varying. This is ascribed to the superposition of varying boundary conditions (mainly river discharge) and their impact on the estuarine circulation. For low settling velocities ($w_s \leq$ 0.1 mm/s), a residual sediment export is modelled in the magnitude of the suspended sediment load of the river and no ETM establishes in the model. In general, this behaviour can be explained by the dynamic balance between the applied settling velocity and the modelled turbulent vertical exchange in the water column.

Furthermore, the sensitivity of the specified sediment concentration at the sea boundary ($ssc_{BC,sea}$) on the sediment import and ETM formation was tested. Figure 7b shows the

Fig. 5 Illustration of resulting estuarine circulation and mixing asymmetries from model results (S0346) at cross section km 55 and 75. **a** Resulting horizontal orthogonal velocity component in ebb direction vhn, with salinity isohalines sa (both averaged for 572 tides, Feb. to Nov. 2009), z_m denoting the average height of the σ-layer. **b**, **c** Vertical channel profiles of turbulent (eddy) diffusivity k_v with water depth (wd) and depth averaged horizontal orthogonal velocity component v2Dn (positive = ebb flow) at km 75 (**b**) and km 55 (**c**), H denoting relative water depth (Hesse 2018)
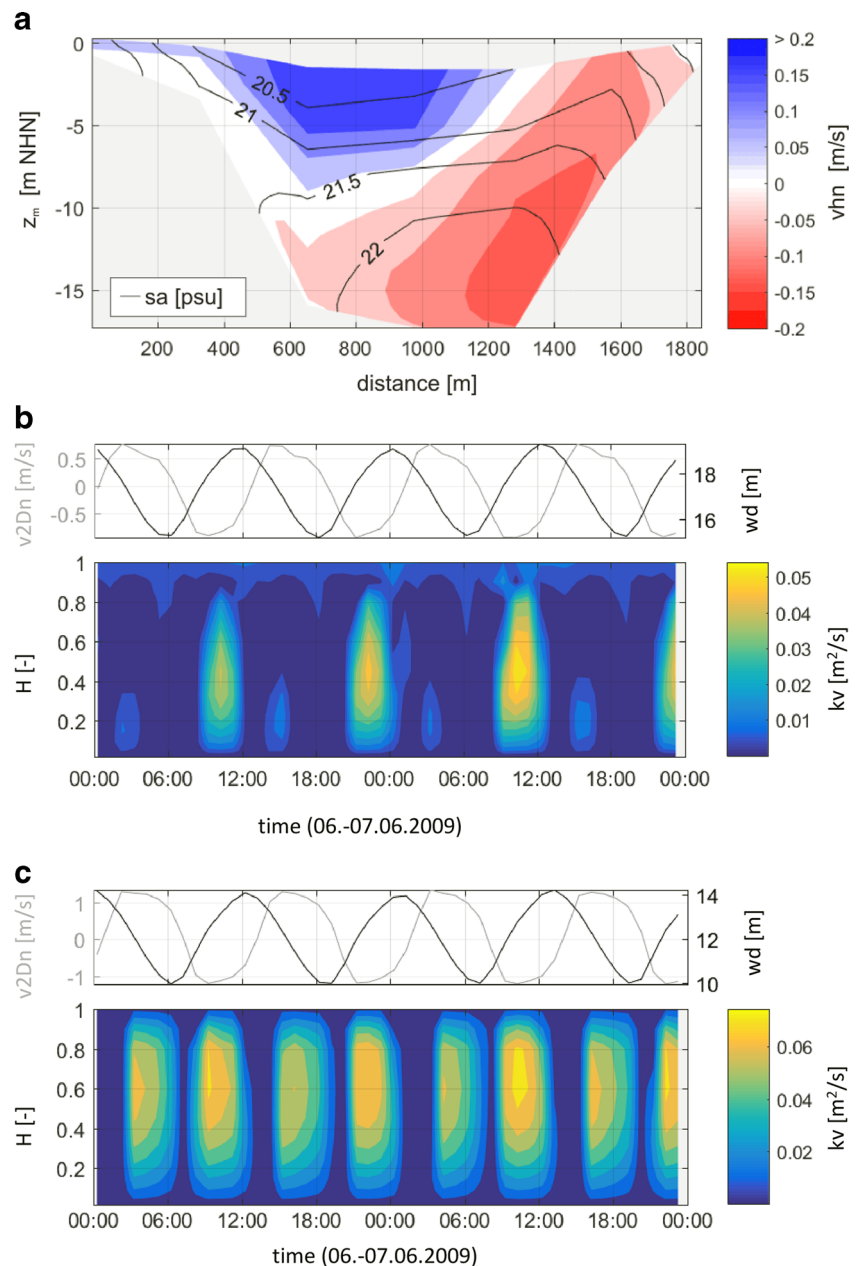
resulting transport for different boundary concentrations and a settling velocity $w_s = 2$ mm/s. For low sea boundary concentrations, the import is reduced ($ssc_{BC,sea} < 0.1$ kg/m^3), but for further increasing concentrations ($ssc_{BC,sea} \geq 0.1$ kg/m^3) the import converges to a maximum, is not increased further and the resulting concentration levels at the ETM are almost identical (as shown for station BAL, S0346 in Fig. 8). This indicates that the total capacity of the residual transport into the estuary is reached. Thus, for low sediment concentrations at the boundary, the import is limited by sediment availability, but for sufficiently high concentrations, the import is limited by the transport capacity and the ETM is not affected by the boundary conditions anymore.
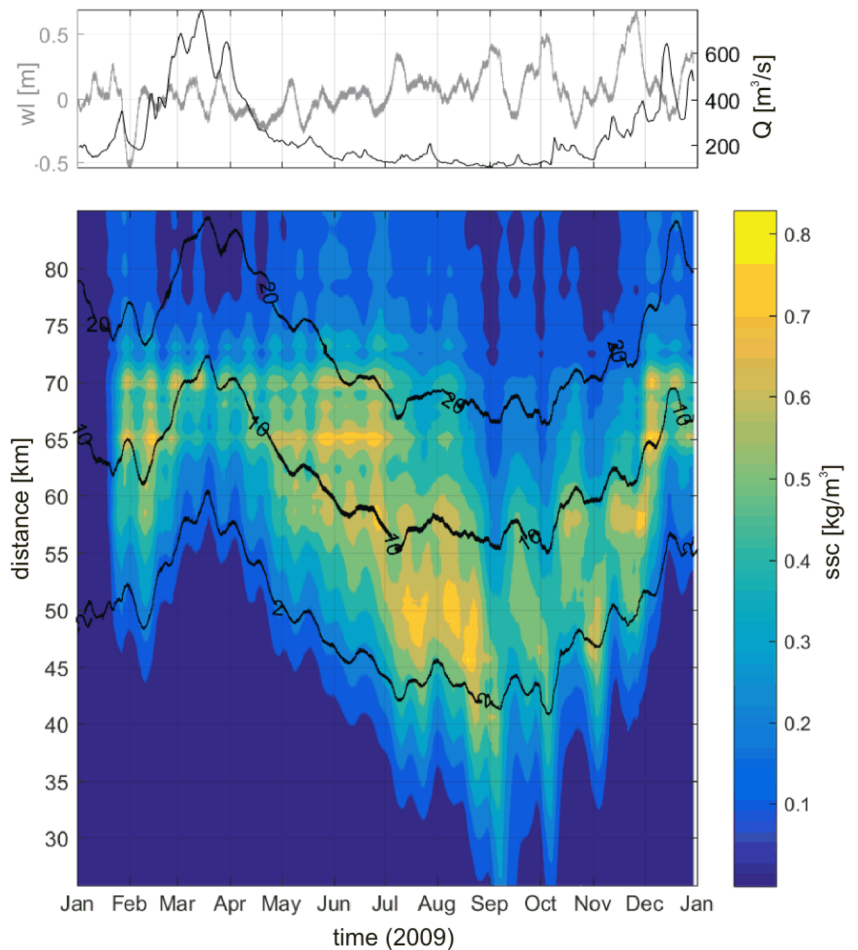
For a settling velocity $w_s = 2.0$ mm/s (S0346), a net sediment import in the same magnitude as the dredging volumes is computed. A stable ETM in the order of measured concentration levels is establishing. It is shifting due to the seasonal river discharge and is modulated by the variation of the tides (Figs. 6, 8, 9 and 10). The location and intensity (mean concentration level) is in accordance with the description in other studies (Kösters et al. 2014; Kappenberg and Grabemann 2001; Grabemann et al. 1997) and available turbidity measurements. Figure 8 shows the average (Feb. to Dec.) and tidally averaged modelled and measured equivalent concentration of turbidity measurements at five monitoring stations (initial phase and data gaps are excluded for the total average). The average longitudinal ETM

Table 2 Presented datasets of simulations and measurements

Scenario	Description
M0001	Measurements of equivalent ssc (WSV 2015)
S0346 (reference run)	$w_s = 2.0$ mm/s
	$scc_{BC,sea} = 0.1$ kg/m³
S0429	Restart with initial condition at end of S0346
S0375	$w_s = 5.0$ mm/s
S0404	3.0 mm/s
S0347	1.0 mm/s
S0436	0.5 mm/s
S0437	0.1 mm/s
S0442	$scc_{BC,sea} = 0$ kg/m³
S0445	0.01 kg/m³
S0446	0.03 kg/m³
S0375	0.20 kg/m³
S0379	0.30 kg/m³
S0443	$sa_{BC,river} = 32$ ppt

location (Fig. 8a) as well as the tidally averaged seasonal variation (Fig. 8b) can be reproduced fairly well, taking into account that no initial sediment distribution was specified in the model

and that the boundary concentration is considerably lower ($ssc_{BC,sea} = 0.1$ kg/m³; $\overline{scc_{BC,river}} \approx 0.05$ kg/m³). On the river side of the ETM, the measurements are underestimated and on the seaward side the measurements are overestimated on average. This indicates a slight seaward shift of the modelled average ETM position. Figure 8b shows the tidally averaged seasonal variation at the monitoring stations: the seasonal shift of the ETM in terms of tidally averaged variation of equivalent turbidity along the channel can be reproduced. Temporarily, the model overestimates the local concertation, but the main shift upstream according to the river discharge can be seen clearly in the measurements as well as in the model results. The average seasonal concentration levels are fairly well met. Besides this, the observed intermediate variations are reproduced qualitatively well and can be ascribed to the spring-neap variations. A strict assignment to specific factors is not made due to the complexity of the realistic boundary conditions which allow for a superposition of several hydrological and meteorological impacts at the same time.

The independence of initial conditions is demonstrated by simulation S0429 (Fig. 8b). This run uses the computed sediment distribution of S0346 as initial conditions and shows an identical behaviour after approximately 1 month.

Fig. 6 Modelled relationship between ETM, salinity and hydrological boundary conditions, shown by suspended sediment concentration (ssc) with salinity isohalines sa (both depth averaged) over time along the river channel, with water level (wl) at the sea (all, 7 days moving mean) and daily discharge Q at the river boundary (Hesse 2018)

Fig. 7 Modelled cumulated total sediment transport (12.5 h moving mean) over time through cross section km 72 (positive = import) for **a** different constant settling velocities w_s (fixed sea boundary concentration ssc = 0.1 kg/m^3) and **b** for different sea boundary concentrations ssc (fixed settling velocity w_s = 2 mm/s) (adapted from Hesse 2018)
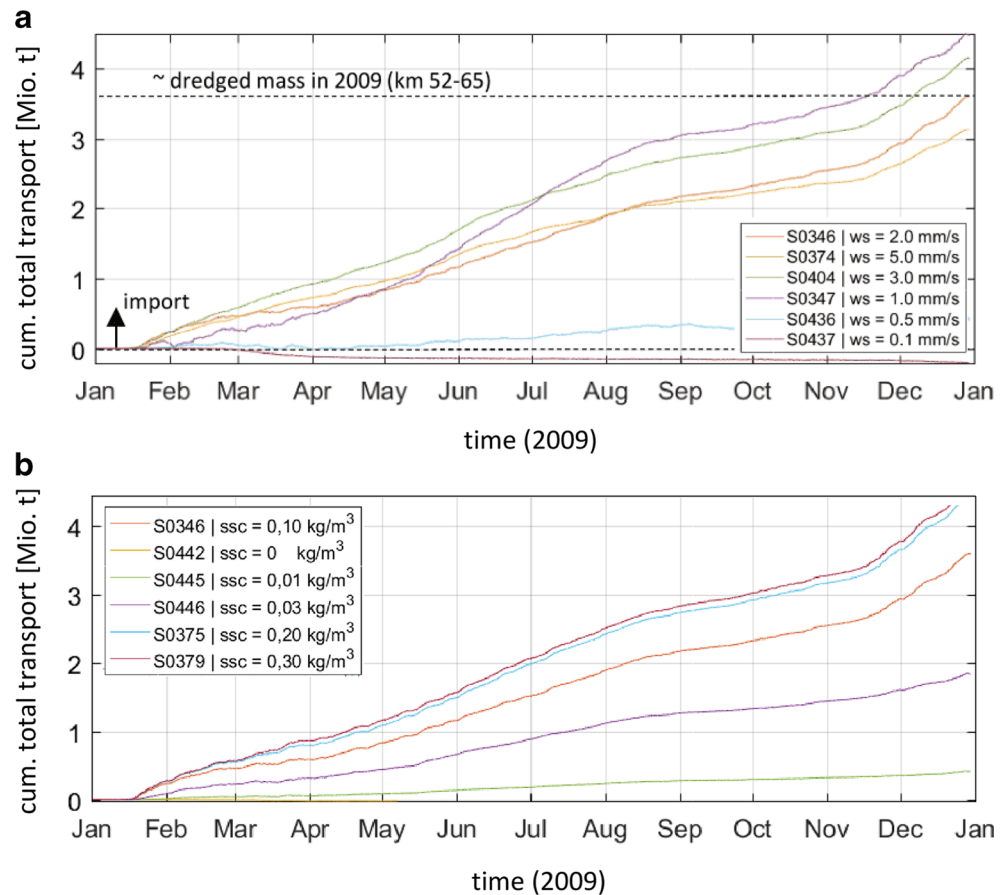
A time series of sediment concentrations for 4 days in October is exemplarily shown in Figs. 9 and 10. Even intra-tidal patterns can be reproduced quite well at different stations in spite of the simplified transport properties. The characteristic patterns of the sediment concentration during the tidal cycle can be seen in the model results as well as in the measurements (Fig. 10). The local sediment dynamics (Fig. 10) can be explained and understood essentially by the ETM dynamics shown in Fig. 9. The intra-tidal ssc patterns are strongly controlled by the location of the ETM, rather than the local flow velocities (comp. Fig. 10). This is in accordance with measurement campaigns in the 1980s in the Weser (Fanger 1986; Rietmöller et al. 1988) analysed by Grabemann (1991), Grabemann and Krause (1989), who analysed the local sediment dynamics at different measurement locations in the estuary. The local patterns are described as the result of resuspension in the adjacent reach ahead from the flow direction, the advection of the ETM, the depletion of the available local sediment source and the anew deposition during the following slack water. Thus, they differ between flood and ebb flow for all stations not located in the very centre of the ETM. For changed river discharges, these patterns remain, but are shifted spatially to the corresponding position within the shifted ETM location. In general, these patterns can be reproduced in the model qualitatively even for other time periods (not shown),

when the average concentration level is temporarily overestimated by the model as shown in Fig. 8.

The resulting sedimentation (accumulation of deposited sediment in the bed layer) after the simulation period of 1 year is presented in Fig. 11. Sedimentation is intensified in deeper channel in the reach of the modelled ETM. This can be explained by the modelled sediment availability, due to ETM formation, subsequent high deposition flux in deeper parts during slack water and consequently high sedimentation rates into the bed layer. As mentioned above, there is a slight seaward shift of the modelled mixing zone and correspondingly the average ETM position. Thus, the modelled core sedimentation area (km 60 to 73) is also shifted seaward from the observed dredging hotspot (km 52 to 65) by approximately 8 km. In other reaches of the navigation channel, no considerable sedimentation of the characteristic fraction occurs in the model.

Finally, two variations of boundary values were tested to underline the correct formation process of the ETM (Fig. 12). If the salinity boundary values of river and sea are equal, no mixing zone is present (S0442) and hence, no ETM establishes in the model. If no primary sediment source is provided at the sea boundary (S0443; compare Fig. 7b), only a very small ETM established, which can be explained by the low river sediment load. The two simulations together give
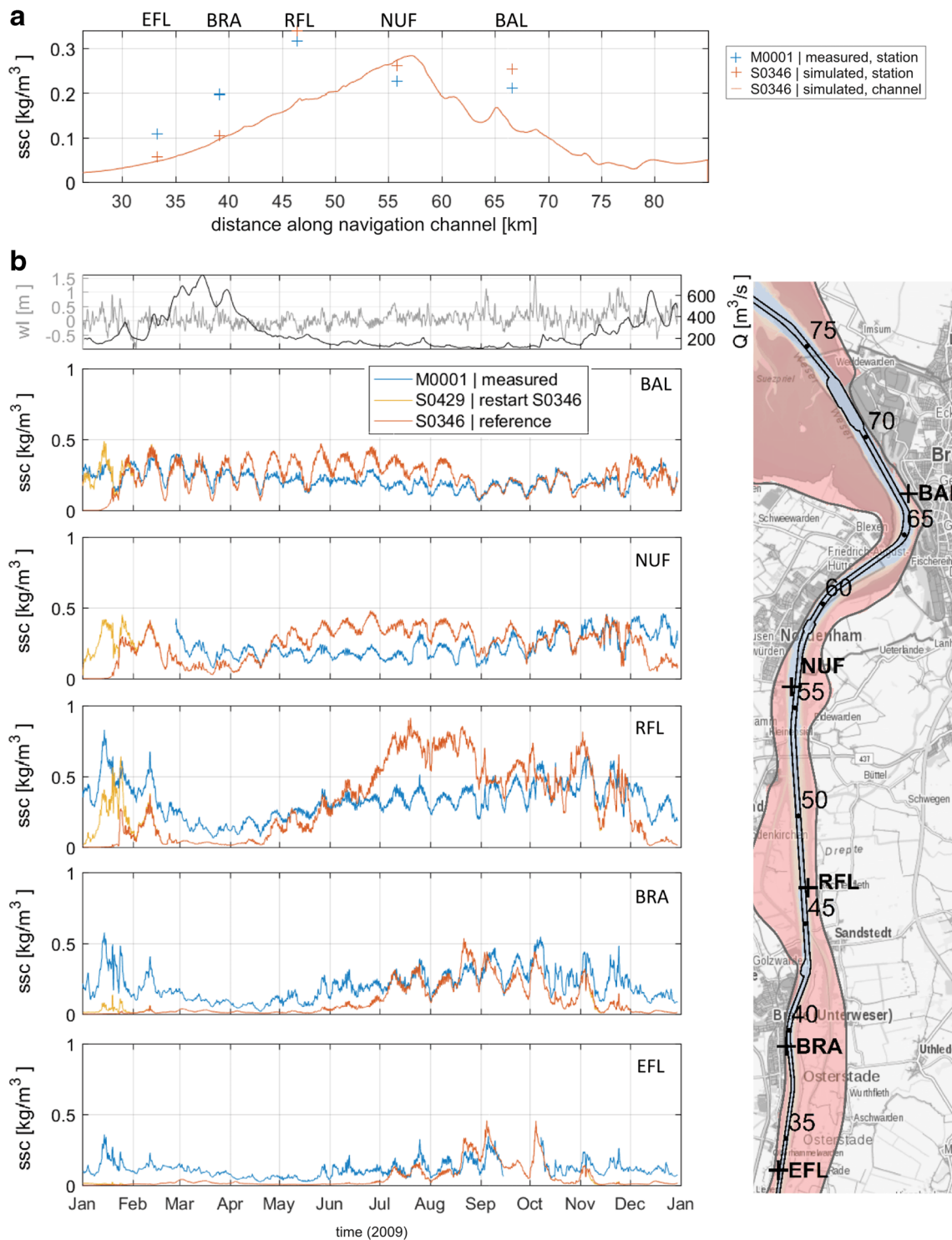
Fig. 8 Comparison of modelled and measured (WSV 2015) suspended sediment concentration (ssc) at 3 m below NHN. **a** Along the channel (averaged Feb. to Dec. 2009) and **b** over time, with water level (wl) at the sea and discharge Q at the river boundary (*all, 12.5 h moving mean*); station names indicated in the right panel (adapted from Hesse 2018)

evidence that the modelled realistic ETM (S0346) is the result of the residual transport from the sea induced by the salinity gradient.

5 Discussion

The model can reproduce the ETM formation by a dynamic equilibrium, which was the objective of the chosen approach:

Fig. 9 Modelled intra-tidal patterns of suspended sediment concentration (ssc) (at 3 m below NHN) and salinity isohalines sa (depth averaged; adapted from Hesse 2018)
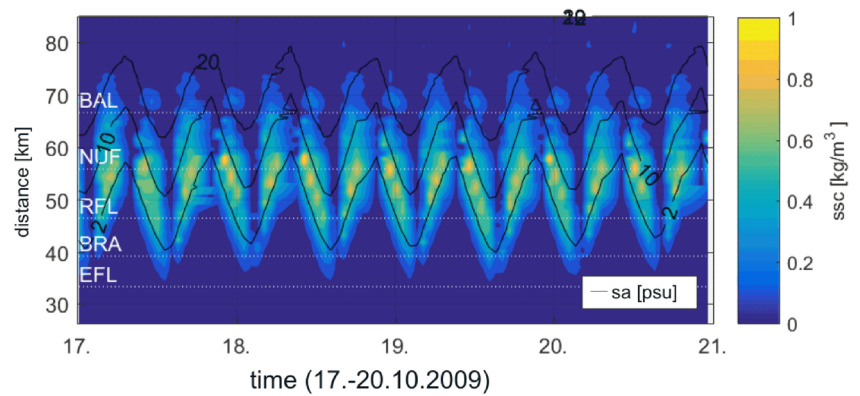
sediment is imported from the outer estuary into the inner estuary due to estuarine circulation and tidal asymmetries. Subsequently, accumulation occurs, leading to an increase of sediment concentration and ETM generation as well as sedimentation due to the high sediment availability and deposition fluxes.
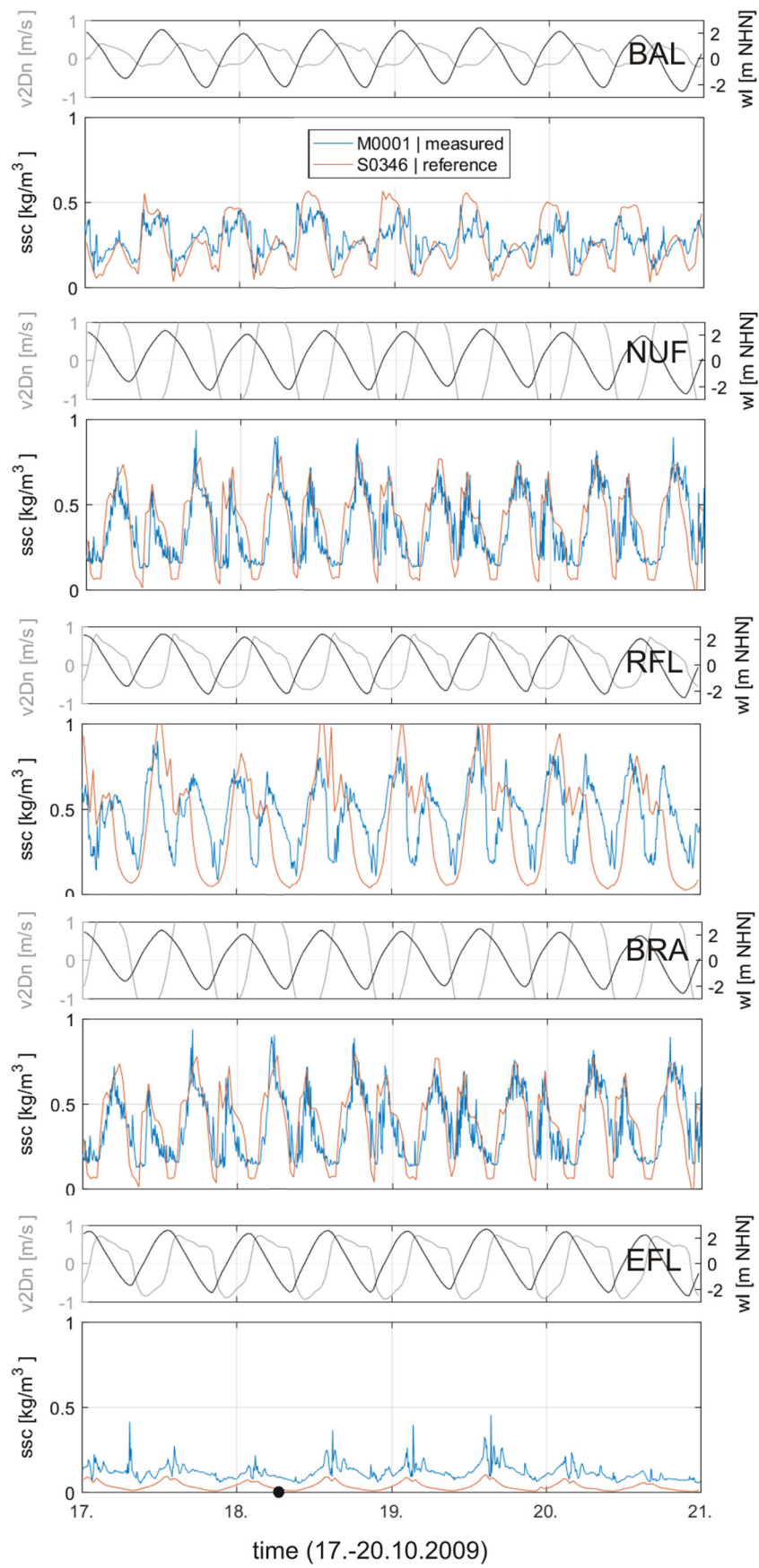
The modelled estuarine circulation with residual flood directed flow in the lower part of the channel as well as tidal asymmetries seems plausible. However, these cannot be validated as adequate measurements are not available. The dynamic salinity distribution can be reproduced in comparison to measurements. Although there is no proof for the estuarine circulation and tidal asymmetries being the main drivers of the sediment import in the Weser estuary, this hypothesis is in accordance with published reviews and detailed studies on the formation mechanisms of the ETM (Geyer and MacCready 2014; Burchard et al. 2018; Burchard and Hetland 2010). The resulting ETM shows a realistic behaviour with regard to the seasonal variation in comparison to available equivalent turbidity measurements (Figs. 8, 9 and 10). The settling velocities, which lead to a considerable residual import ($w_s = 1.0...5.0$ mm/s) according to Fig. 7a, are in the range of settling velocities of macroflocs measured in the Ems estuary (van Leussen 2011). According to van Leussen, the settling of macroflocs is very important for the deposition mass flux and consequently plays a key role in the tidal erosion-deposition cycles. These cycles can be referred to as "building blocks" for the residual fine sediment transport (van Leussen 2011).

The impact of the sediment availability at the sea boundary (Fig. 7b) indicates that the sediment import is limited either by the residual transport capacity due to estuarine circulation and tidal asymmetries or the sediment availability in the North Sea. It cannot be determined by these model results which effect is controlling the import in nature. Both limitations could have an impact for different conditions. However, the model results show that the capacity of the residual transport can control the accumulation and ETM formation if sufficient sediment is available at the sea.

The local measured characteristic pattern (Fig. 10) can be explained quite well by the modelled horizontal advection, vertical deposition, resuspension of sediment during the tidal cycle and the relative position in the ETM (Fig. 10). According to Grabemann (1991), the characteristic patterns (Fig. 10) can be essentially explained by the relative position of the monitoring station within the reach of the shifting ETM (compare Fig. 9). The model reproduces these characteristic patterns qualitatively well, though the quantitative intra-tidal variation can only partly be reproduced.

These observed deviation between measurements and model on the tidal scale can be explained by flowing aspects: as mentioned in Section 2, the sediment settling and bed exchange are deliberately parametrized in a simplified way. The vertical distribution is likely not to be reproduced with the model and cannot be analysed as no vertically resolved measurements are available. The shown deviations of model results and measurements at one depth on the intra-tidal time scale might be mainly ascribed to the application of one constant settling velocity as well. The underestimation in times of the absence of the ETM at one location can be related to the usage of one model fraction only. A background concentration in terms of wash load is not taken into account. More fractions or a more complex settling parameterization would be desirable. However, that would make calibration very challenging with regard to the global sediment transport which leads to the increased concentration levels at the ETM dynamically. Especially a settling formulation with a concentration dependency would be difficult to apply due to the global *and* local impact of the settling velocity for a given bed exchange (compare Figs. 6, 7, 8, 9 and 10). One specific constant settling velocity (e.g. $w_s \neq 2$ mm/s) for a fixed bed exchange parameter setting does not lead by default to *both* a correct magnitude of the import (Fig. 7a) in comparison to observed

Fig. 10 Comparison of measured (WSV 2015) and modelled intra-tidal ▶ patterns of suspended sediment concentration (ssc) for different stations at 3 m below NHN, with modelled water level (wl) and depth averaged current velocity v2Dn; station names indicated in Fig. 8 (adapted from Hesse 2018)
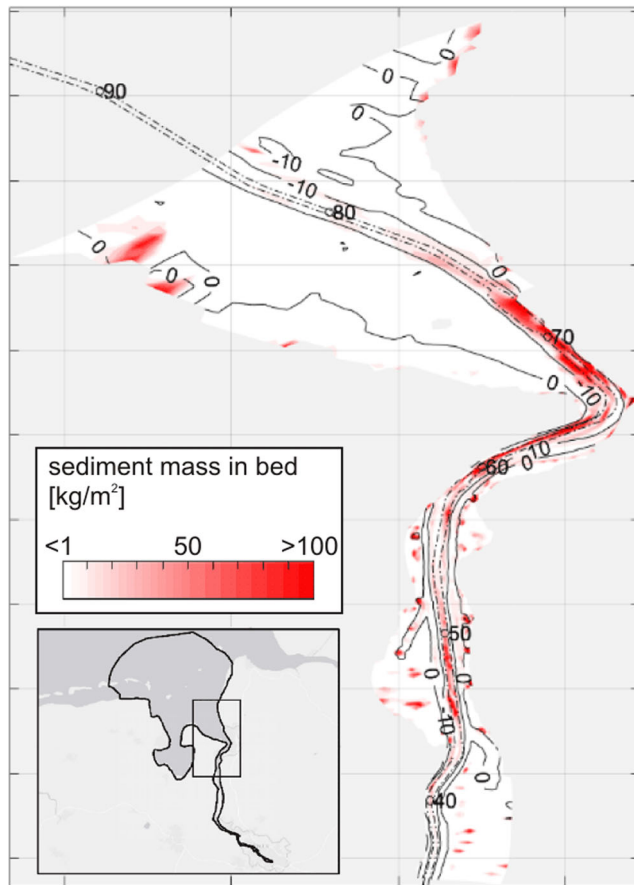
Fig. 11 Modelled sedimentation (accumulated sediment mass in bed layer) after 1 year (2009) with bathymetry contours below chart datum (0, −10 m NHN) and navigation channel (distorted spatial view; adapted from Hesse 2018)

the average sediment concentration levels and turbidity levels respectively to show the general seasonal behaviour.

In spite of the discussed occurring local and temporary short-term deviations, the presented model shows in general the intended large-scale behaviour for the averaged seasonal sediment dynamics. The modelled import of sediment leads to an accumulation, which generates a dynamical local secondary sediment source according to the supply-limited approach. The available sediment is resuspended by tidal forcing, leading to an increased sediment concentration in the accumulation zone and the dynamic formation of an ETM. The high concentration leads to an increased deposition flux, which explains the observed sedimentation in nature. The dimensionless fluff layer of the 2-Layer-Concept enables the reproduction of the short-term bed exchange fluxes and residual import as well as net deposition for longer periods. The fixed bed is used to buffer the "excess" sediments in the ETM, which are dredged in nature. This enables the reproduction of the dynamic equilibrium in the model for the current setup. In addition, the local bed exchange is simplified with regard to the model resolution and processes scale. The exchange of the lower bed layer leads to rather depositional conditions, though the deposition depends on sediment availability. Anyway, the actual bed exchange cannot be derived with the current model setup due to the intensive dredging measures, which are not considered here, but extract sediment from the ETM in nature. For the composition of the available measured turbidity, it cannot be differentiated between the proportion of the longitudinal ETM advection and of the local resuspension of mud (fluff layer) or of the erosion of more stable deposits (bed layer). This exchange might be varying especially between the spring or neap conditions. Besides, in some areas, local bed forms lead to different entrainment behaviour of the mud layer in nature (Becker 2011). This process is not resolved in the model either, but might have an effect on the local resuspension and characteristic sediment dynamics. The actual impact of the bed forms on the regional sediment dynamics at the ETM cannot be quantified so far. Besides, it is likely that the deposition in shallow areas might be rather overestimated due to the bed exchange formulation and the neglecting of waves.

dredging *and* correct local concentration levels in comparison to measured turbidity (Figs. 9 and 10). In fact, this is highly dependent on the balance between the bed exchange parameters and settling velocity as well as modelled vertical mixing and residual current. In addition, as mentioned before, the measured turbidity might not fully represent the actual concentration in nature during the tidal cycle due to the used constant conversion factor. Anyway, tidally averaged time series should be rather comparable with regard to variation of

Fig. 12 Time and depth averaged ssc along a length section (57 tides, in March) for different boundary values: reference scenario S0346, $ssc_{sea} = 0.1$ kg/m^3; S0442, $ssc_{sea} = 0$ kg/m^3; S0443, $sa_{river} = 32$ ppt $\approx sa_{sea}$ (adapted from Hesse 2018)
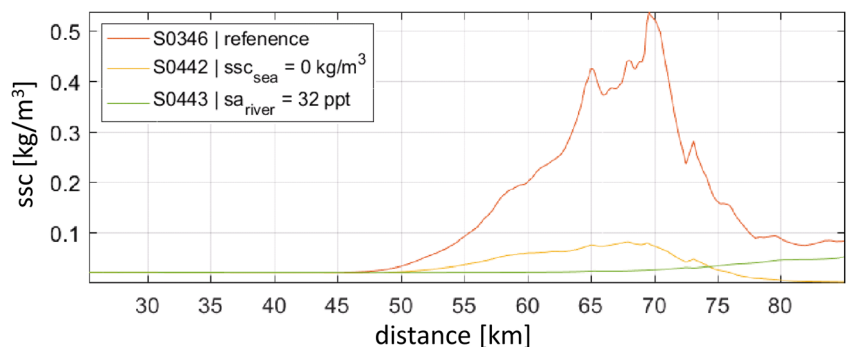
The consideration of the impact of waves on the shear stress might lead to more realistic higher shear stresses in these areas and a lower net deposition especially in the outer estuary.

Furthermore, the comparison of averaged measured and modelled seasonal salinity and ssc indicate that the modelled mixing zone and ETM is slightly shifted seawards on average or that the shifting is delayed respectively. The shift of the average ETM location might also partly explain the temporal seasonal local deviations between measurements and model results as well as the shifted core sedimentation area in comparison with the observed dredging hotspot. From a process-oriented point of view, this confirms the ETM-generation process by residual transport due to the salinity gradient in the model. This is in line with the sensitivity analysis of the primary sediment source at the sea: if sufficient sediment is available, the residual transport capacity according to the establishing transport mechanisms seems to control the sediment import and accumulation. It has been proven by variation of the boundary values (Fig. 12) that the ETM formation is only occurring in the model, if a mixing zone is present and if there is a sufficient sediment source at the sea. If dredging and dumping was considered, the specified magnitude ($ssc_{BC,sea} \geq 0.1$ kg/m^3) could be lower as the sediment which is dredged in the ETM would be available to the system again by the dumping it in the outer estuary. The shown modelled sediment fluxes from the outer into the inner estuary are expected to be comparable in this case. These analyses demonstrate that the ETM is the result of a dynamic equilibrium as stated in the objectives. The ETM is formed dynamically by sediment import due to the modelled hydrodynamic processes and salt distribution. The dynamic import enables the reproduction of the measured turbidity levels *and* the observed magnitude of net deposition in terms of dredged sediment mass.

6 Conclusion

A new model approach is presented which enables the efficient simulation of the seasonal sediment dynamics and sedimentation in the presence of an estuarine turbidity maximum (ETM). A 3D model of the Weser estuary with realistic boundary conditions is used to test this approach and to compare the achieved model results with actual measurements and dredging volumes. The combination of large-scale sediment transport in terms of a supply-limited approach (van Maren et al. 2011) and simplified sediment transport properties allow the reproduction of residual sediment transport, formation of the ETM and subsequent sedimentation. Only one characteristic fraction with a constant settling velocity as well as an extended parameterized bed exchange formulation (2-Layer-Concept; van Kessel et al. (2011)) is applied. The focus of the modelling approach lies on the reproduction of the seasonal sediment dynamics in terms of sediment balances and the seasonal variation of tidally averaged sediment concentration.

The vertical distribution of ssc and the actual bed structure are chosen not to be modelled in detail. The simplified parametrization enables efficient calibration and simulation with passable computational effort.

The seasonal variations at different monitoring stations within the reach of the shifting ETM can be reproduced fairly well taking into account that no initial sediment distribution is specified. The position of the modelled ETM is shifting depending on the river discharge and is modulated by tidal variation in accordance with measurements. The observed time-resolved characteristic sediment dynamic pattern at one location can be explained well by the modelled ETM advection, deposition and resuspension during the tidal cycle. The magnitude of sedimentation in comparison to dredged sediment amounts can be reproduced in the reach of the ETM. The model reproduces the ETM formation independently from the initial conditions. A dynamic equilibrium is establishing between modelled sediment import, increased sediment concentrations and generation of the ETM respectively as well as sedimentation within the reach of the ETM.

The residual import can be explained by the modelled residual transport mechanisms which establishes in the model due to the three-dimensional modelled tidal flow as well as salt transport and distribution. Sediment is transported into the estuary due to a residual flood directed flow in the lower part of the channel (estuarine circulation) and due to tidal asymmetries. The corresponding accumulation leads to the formation of an ETM in the model. Without the modelled mixing zone or without an adequate sediment source at the sea boundary, no ETM is developing in the model which confirms the formation mechanism. The residual transport strongly depends on the sediment properties, such as the specified settling velocity.

Summing up, the formation of the ETM can be referred to the successive tidal resuspension-deposition cycles and the balance between settling velocity and modelled turbulent diffusivity according to the sediment transport equation, leading to residual transport and accumulation. Thus, the model explains the observed seasonal variation as well as the magnitude of dredging by a process-based approach with a simplified sediment settling and extended bed exchange. That leads to a stable ETM formation and sedimentation due to an establishing dynamic equilibrium in the model.

References

Allen GP, Salomon JC, Bassoullet P, Du Penhoat Y, de Grandpre C (1980) Effects of tides on mixing and suspended sediment transport in macrotidal estuaries. *Sediment Geol* 26(1980):S. 69–S. 90 graph. Darst

BAW (2012). Validierung des Jade-Weser-Basismodells 2012 für das Verfahren UnTRIM2007-SediMorph: Teilbericht 1: Hydrodynamik und Salztransport (BAW-Bericht B3955.02.10.10048.1-4, in preparation), Bundesanstalt für Wasserbau

Becker, M. (2011). Suspended sediment transport and fluid mud dynamics in tidal estuaries, Dissertation, Bremen, University Bremen

Berlamont J, Ockenden M, Toorman E, Winterwerp J (1993) The characterisation of cohesive sediment properties. Coast Eng 21(1–3): 105–128

BfG (2014a). Produktblatt: ALS-Befliegungen Unter-/Außenweser 2012-2015: Produkt: Digitales Oberflächenmodell (DOM) 2012

BfG (2014b). Sedimentmanagementkonzept Tideweser: Untersuchung im Auftrag der WSA Bremen und Bremerhaven, Bericht 1794, Koblenz

Black KS, Tolhurst TJ, Paterson DM, Hagerthey SE (2002) Working with natural cohesive sediments. J Hydraul Eng 128(1):2–8

Brenon I, Le Hir P (1999) Modelling the turbidity maximum in the seine estuary (France). Identification of formation processes. Estuar Coast Shelf Sci 49(4):525–544

Burchard H, Hetland RD (2010) Quantifying the contributions of tidal straining and gravitational circulation to residual circulation in periodically stratified tidal estuaries. J Phys Oceanogr 40(6):1243–1262

Burchard H, Schuttelaars HM, Ralston DK (2018) Sediment trapping in estuaries. Annu Rev Mar Sci 10(1):371–395

van der Wegen M, Jaffe BE, Roelvink JA (2011) Process-based, morphodynamic hindcast of decadal deposition patterns in San Pablo Bay, California. J Geophys Res 116(F2):1856–1887. https://doi.org/10.1029/2009JF001614

Downing J (2006) Twenty-five years with OBS sensors. The good, the bad, and the ugly. Cont Shelf Res 26(17):2299–2318

DWD (2013). Wind measurement at station Alte Weser, Deutscher Wetterdienst

Dyer KR (1973) Estuaries: a physical introduction. A Wiley-Interscience Publication, Wiley, London

Dyer KR (1988), Fine sediment particle transport in estuaries, in Dronkers J and van Leussen W (Eds.), Physical processes in estuaries: [papers presented at an International Symposium on Physical Processes in Estuaries, held Sept. 9–12, 1986, in the Netherlands], Springer, Berlin, pp. 295–310

Fanger HU (1986). MASEX '83, eine Untersuchung über die Trübungszone der Unterweser, GKSS, 86/E/6, GKSS-Forschungszentrum, Geesthacht

Geyer WR, MacCready P (2014) The estuarine circulation. Annu Rev Fluid Mech 46(1):175–197

Grabemann I. (1991). Die Trübungszone im Weser-Ästuar: Messungen und Interpretation, Dissertation, Hamburg, Universität Hamburg

Grabemann I, Krause G (1989) Transport processes of suspended matter derived from time series in a tidal estuary. J Geophys Res 94:14373

Grabemann I, Krause G (2001) On different time scales of suspended matter dynamics in the Weser estuary. Estuaries 24(5):688–698

Grabemann I, Kappenberg J, Krause G (1995) Aperiodic variations of the turbidity maxima of two German coastal plain estuaries. Neth J Aquat Ecol 29(3–4):217–227

Grabemann I, Uncles RJ, Krause G, Stephens JA (1997) Behaviour of turbidity maxima in the Tamar (U.K.) and Weser (F.R.G.) estuaries. Estuar Coast Shelf Sci 45(2):235–246

Grabowski RC, Droppo IG, Wharton G (2011) Erodibility of cohesive sediment: the importance of sediment properties. Earth Sci Rev 105(3–4):101–120

Grasso F, Verney R, Le Hir P, Thouvenin B, Schulz E, Kervella Y, Khojasteh Pour Fard I, Lemoine J-P, Dumas F, Garnier V (2018) Suspended sediment dynamics in the macrotidal seine estuary (France). 1. Numerical modeling of turbidity maximum dynamics. J Geophys Res Oceans 123(1):558–577

Hesse RF (2018). Zum Transportverhalten kohäsiver Sedimente in Ästuaren, Dissertation, in progress, Technische Universität Hamburg

Heyer H and Schrottke K (2013). Aufbau von integrierten Modellsystemen zur Analyse der langfristigen Morphodynamik in der Deutschen Bucht AufMod: Gemeinsamer Abschlussbericht für das Gesamtprojekt mit Beiträgen aus allen 7 Teilprojekten

Holliday CP, Rasmussen TC and Miller WP (2003), Establishing the relationship between turbidity and total suspended sediment concentration, Proceedings of the 2003 Georgia Water Resources Conference

Jay DA, Musiak JD (1994) Particle trapping in estuarine tidal flows. J Geophys Res 99:445–461

Kappenberg J, Grabemann I (2001) Variability of the mixing zones and estuarine turbidity maxima in the Elbe and Weser estuaries. Estuaries 24(5):699

van Kessel T, de Boer G and Boderie P (2009). Calibration suspended sediment model Markermeer

van Kessel T, Winterwerp H, van Prooijen B, van Ledden M, Borst W (2011) Modelling the seasonal dynamics of SPM with a simple algorithm for the buffering of fines in a sandy seabed. Cont Shelf Res 31(10):124–134

Kösters F, Grabemann I and Schubert R (2014), On SPM dynamics in the turbidity maximum zone of the Weser estuary, in Kuratorium für Forschung im Küsteningenieurwesen (Ed.), Die Küste: Archiv für Forschung und Technik an der Nord- und Ostsee ; Archive for Research and Technology on the North Sea and Baltic Coast, Modelling, 81 (2014), pp. 393–408

Lang G (1990). Zur Schwebstoffdynamik von Trübungszonen in Ästuarien, Dissertation, Hannover, Universität Hannover

Lange D, Müller H, Piechotta F and Schubert R (2008), The Weser Estuary, in Kuratorium für Forschung im Küsteningenieurwesen (Ed.), Die Küste: Archiv für Forschung und Technik an der Nord- und Ostsee ; Archive for Research and Technology on the North Sea and Baltic Coast, ICCE, Vol. 74, pp. 275–287

Le Hir P, Cayocca F, Waeles B (2011) Dynamics of sand and mud mixtures. A multiprocess-based modelling strategy. Cont Shelf Res 31(10):S135–S149

Lesser GR, Roelvink JA, van Kester JATM, Stelling GS (2004) Development and validation of a three-dimensional morphological model. Coast Eng 51(8):883–915

van Leussen W (1994) Estuarine macroflocs and their role in fine-grained sediment transport, Dissertation, Universiteit Utrecht, Faculteit Aardwetenschappen, Ministry of Transport, Public Works and Water Management, Directorate-General of Public Works and Water Management, Den Haag. ISBN 90-393-0410-6

van Leussen W (2011) Macroflocs, fine-grained sediment transports, and their longitudinal variations in the Ems estuary. Ocean Dyn 61(2–3): 387–401

Malcherek A (1995). Mathematische Modellierung von Strömungen und Stofftransportprozessen in Ästuaren, Dissertation, Hannover, Institut für Strömungsmechanik und Elektronisches Rechnen im Bauwesen der Universität Hannover

van Maren DS, Winterwerp JC, Decrop B, Wang ZB, Vanlede J (2011) Predicting the effect of a current deflecting wall on harbour siltation. Cont Shelf Res 31(10, Supplement):S182–S198

van Maren DS, van Kessel T, Cronin K, Sittoni L (2015) The impact of channel deepening and dredging on estuarine sediment concentration. Cont Shelf Res 95:1–14

Maushake C and Grünler S (2015), personal communication

Mueller A, Puls W (1996) Modelling of suspended matter transport in tidal rivers. Adv Limnol 47(1996):S.343–S.351 96/E17

Papenmeier S, Schrottke K, Bartholomä A, Flemming BW (2013) Sedimentological and rheological properties of the water–solid bed interface in the Weser and Ems estuaries, North Sea, Germany. Implications for fluid mud classification. J Coast Res 289:797–808

Pejrup M, Mikkelsen OA (2010) Factors controlling the field settling velocity of cohesive sediment in estuaries. Estuar Coast Shelf Sci 87(2):177–185

Rietmöller R, Fanger H-U, Grabemann I, Krasemann, HL, Ohm K, Böning J, Neumann LJR, Lang G, Markofsky M and Schubert R (1988), Hydrographic measurements in the turbidity zone of the Weser estuary, in Dronkers J and van Leussen W (Eds.), Physical processes in estuaries: [papers presented at an International Symposium on Physical Processes in Estuaries, held Sept. 9–12, 1986, in the Netherlands], Springer, Berlin

Sanford LP (2008) Modeling a dynamically varying mixed sediment bed with erosion, deposition, bioturbation, consolidation, and armoring. Comput Geosci 34(10):1263–1283

Schrottke K, Becker M, Bartholomä A, Flemming BW, Hebbeln D (2006) Fluid mud dynamics in the Weser estuary turbidity zone tracked by high-resolution side-scan sonar and parametric sub-bottom profiler. Geo-Mar Lett 26(3):185–198

Schulz E, Grasso F, Le Hir P, Verney R, Thouvenin B (2018) Suspended sediment dynamics in the macrotidal seine estuary (France). 2. Numerical modeling of sediment fluxes and budgets under typical hydrological and meteorological conditions. J Geophys Res Oceans 123(1):578–600

Simpson JH, Brown J, Matthews J, Allen G (1990) Tidal straining, density currents, and stirring in the control of estuarine stratification. Estuaries 13(2):125–132

Winterwerp JC (2002) On the flocculation and settling velocity of estuarine mud. Cont Shelf Res 22(9):1339–1360

Winterwerp JC, van Kesteren WGM (eds) (2004) Introduction to the physics of cohesive sediment in the marine environment, Developments in sedimentology, Vol 56, 1 ed., Elsevier, Amsterdam. ISBN 0444515534

(WSV: Wasser- und SchifffahrtsVerwaltung des Bundes) (2014) River runoff, salinity and suspended sediment concentration measurement at station Intschede (INS): provided by (WISKI: Wasserstraßeninformationssystem), Wasserstraßen- und Schifffahrtsverwaltung des Bundes (WSV)

(WSV: Wasser- und SchifffahrtsVerwaltung des Bundes) (2015) Turbidity measurements stations Bremerhaven Alter Leuchtturm (BAL), Nordenham Unterfeuer (NUF), Rechtenfleth (RFL), Brake (BRA), Elsfleth (EFL): provided by (WISKI: Wasserstraßeninformationssystem), Wasserstraßen- und Schifffahrtsverwaltung des Bundes (WSV)